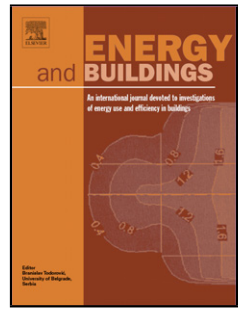

Title: A comparison of heating terminal units: fan-coil versus radiant floor, and the combination of both.

Author: <ce:author id="aut0005" author-id="S0378778816320849-b97c8b8edd0ed77f2c9767138b5e6c38"> Antonio Atienza Márquez<ce:author id="aut0010" author-id="S0378778816320849-d0c5599967ab15cc2aee277adf04681f"> José Manuel Cejudo López<ce:author id="aut0015" author-id="S0378778816320849-389fa7fbebfbdf0236466d59fc262418"> Francisco Fernández Hernández<ce:author id="aut0020" author-id="S0378778816320849-4c8fd7538d695b388a3abe9b4fee70a0"> Fernando Domínguez Muñoz<ce:author id="aut0025" author-id="S0378778816320849-2a457b2a2d4c3174fe9af4c44ce9db21"> Antonio Carrillo Andrés

PII:	S0378-7788(16)32084-9
DOI:	http://dx.doi.org/doi:10.1016/j.enbuild.2016.12.092
Reference:	ENB 7271
To appear in:	*ENB*
Received date:	14-6-2016
Revised date:	3-11-2016
Accepted date:	30-12-2016

A comparison of heating terminal units: fan-coil versus radiant floor, and the combination of both.

Antonio Atienza Márquez*, José Manuel Cejudo López, Francisco Fernández Hernández, Fernando Domínguez Muñoz, Antonio Carrillo Andrés

Energy Research Group, ETSII-University of Málaga

C/Doctor Pedro Ortiz Ramos s/n; 29013 Málaga (Spain)

*Corresponding author: atienza_marquez@uma.es

Highlights

- This paper analyses the operation of a heating system whose terminal units are a radiant floor and a fan-coil, and whose production unit is an air-water heat pump.
- The uncertainty in the part load efficiency of the heat pump was quantified by performing a sensitivity analysis with three different part-load performance curves.
- Four control strategies are defined and compared using a TRNSYS model.
- The energy consumption of the system is mainly influenced by the part load performance of the heat pump, although the differences are small.
- The combined system (radiant floor and fan-coil) shows the best relationship between energy consumption and comfort level.

Abstract

Several control strategies are compared for a hydronic heating system that combines two different terminal units, radiant floor and fan-coil, in the same thermal zone. The performance of the combined system is evaluated in terms of energy consumption and comfort level. The production unit is an air-water heat pump. Four control strategies are defined and compared using a TRNSYS model: one strategy is applied when only the radiant floor operates, two strategies (simply and improved) are applied when only the fan-coil operates, and one strategy is applied when both terminal units operate simultaneously. Simulations are undertaken for three major cities with different heating requirements. In terms of comfort, the combined system achieves the higher scores, ensuring comfort conditions during most of the heating season. In terms of energy consumption, the worst option is the one that uses a fan-coil with fixed air velocity and fixed inlet water temperature. Nonetheless, there are not important differences between the analysed control options. The energy consumption of the system is mainly influenced by the part load performance of the heat pump, although the differences are small.

Nomenclature

C	Capacitance (kJ h^{-1} K^{-1})
Cap	Thermal power at nominal conditions (kW)
COP	Coefficient of Performance
Cp	Specific heat (kJ kg^{-1} K^{-1})
$\dot{m}$	Mass flow rate (kg h^{-1}) or volumetric flow rate: air (m^3 h^{-1}), water (l h^{-1})
PLR	Partial load ratio
$\dot{Q}$	Heat flux (W)
t	Temperature (^{o}C)
$\dot{W}$	Electric consumption

Greek letters

Δ	Temperature difference
δ	Change of the room dry-bulb temperature during six minutes (^{o}C)
ϵ	Effectiveness

Subscripts

a	Air
ct	Catalogue
fan	Fan
max	Maximum
min	Minimum
MR	Mean radiant
O	Outdoor

P	Production
PL	Partial load
R	Air zone
s	Supply air
SP	Set-point
surf	Radiant floor surface
v	Fan speed
w	Water
1	Input
2	Output

1. Introduction

The use of radiant floors for heating is widespread. The main advantages are improved comfort and a lower energy consumption [1] [2]. An important drawback is the higher thermal mass of the floor, which complicates the control of the system. The large thermal inertia can cause delays and overheating, leading to higher energy consumption and dissatisfied occupants. Compared to radiant floors, fan-coils work with higher water temperatures and shorter response times.

This paper examines the integration of radiant floors and fan-coils in the same thermal zone. Despite a higher investment cost, the combination of both terminal units can offer interesting benefits. A good example of this is found in zones with highly variable occupation. During the heating-up phase from the initial state, the use of fan-coils fed with water at 45 ^{o}C helps the system to reach the zone set-point temperature quickly. At the same time, the floor will be gradually increasing its temperature until it is able to deal by itself with the total thermal load. The efficiency of the thermal production unit increases when the floor works alone because of the lower production temperature required (around 35 ^{o}C). In this way, the combined system should improve comfort levels during the first hours of occupancy and reduce the energy consumption during the rest of the time.

Another important benefit of combining both terminal units is to increase the total capacity of the HVAC system. A classic example of this is the operation in cooling mode, where the maximum capacity of the radiant floor is 40-50 W m^{-2} [3] [4] because the risk of condensation limits the floor surface temperature. The concurrent operation of fan-coils makes it possible to satisfy the latent load and the fraction of sensible load that the floor cannot satisfy [5] [6]. Nevertheless, the operation in heating mode has not been studied in depth.

Concerning the control strategies, a good classification can be found in Afram and Janabi-Sharifi [7]. There are many options, ranging from classical controls like on/off or PID, to advanced control methods like model-based predictive (MPC), fuzzy logic or neural networks. However, in our case, the complexity of the control system is not economically justified. The number and type of sensors and actuators are restricted in residential applications, and the "intelligence" of the system is limited. See for instance Marušić and Lončar [8] and Brooks et al. [9], who prove that the energy savings achieved by complex control strategies are not high enough to justify the increased cost.

The control strategies for combined systems use to be quite simple. For example, Backman et al. [10] studied a combined system during a whole year in two different locations in the USA. The fan-coil removed the latent load and complemented the floor when necessary. There was not a "smart" control to optimize the energy consumption. On the other hand, Beghi et al. [11] presented a more complex optimal strategy based on load prediction.

This paper analyses the best operation strategy for a hydronic heating system in which the production system is an air-water heat pump and the terminal units are a radiant floor and a fan-coil. The simplicity of the control system is an important practical restriction. We compare four different control strategies using TRNSYS 17 [12]. All of them must fulfil the following constraints:

- Same production temperature of hot water for both terminal units.
- Constant water flow.
- Control decisions are only based on the zone dry-bulb temperature.

The optimal control strategy must answer the following questions: a) which is the operation priority for each terminal unit, b) what is the set-point temperature for hot water production if each terminal unit needs a different temperature, and c) how to avoid zone overheating when the radiant floor is operating.

2. Description of the system

Figure 1 shows the scheme of the system proposed in this work. Notice that the hydraulic circuit was simplified by replacing the traditional three-way mixing valve, designed to reduce the water temperature entering the floor, by an on-off two-way valve. The controller outputs are: the hot water set-point for the air-water heat pump, the operation signal (on-off) of the circulating pump, the operation signal for the heating floor (on-off of the two-way valve) and, finally, the velocity and operation (on-off of the two-way valve) of the fan-coil.

Figure 1. Scheme of the proposed hydronic heating system: radiant floor coupled with a fan-coil.

2.1 Heat pump model.

We have developed an air-water heat pump model in TRNSYS that is based on two set of curves. With the first set, the COP at full load is calculated from the outdoor and water production temperatures. Figure 2 (a) represents the data for a Daikin Altherma air-water heat pump [13]. These curves include the effect of defrosting cycles. With the second set of curves, we modify the full load COP as function of the part load ratio (PLR). This correction is very important because residential heat pumps predominately operate at part load.

The part load performance of a heat pump depends on numerous factors related to its constructive details (type of compressor, size of the heat exchangers, circuiting, etc.) and the control strategies used to match load and capacity (compressor/s, pump/s and fan/s regulation). Some authors have reported on the effect of some of these factors. According to Safa et al. [14], the use of variable speed compressors improves the efficiency at part load operation in comparison with other technologies. The work of Edwards and Finn [15] proves that using a control strategy that optimizes the water flow improves the system efficiency at partial load. The reference In et al. [16] shows that the type of refrigerant also affects the part load performance.

When it comes to simulate a heat pump, the simulationist usually finds that manufacturers provide little (if any) information on the performance of their products at part load conditions. In order to quantify the effect of this uncertainty, we have defined three different part-load performance curves (see Fig. 2 (b)) that describe the possible trends between the part load COP (COP_{PL}) and the PLR. Curve A Fig. 2 (b) represents equipment with constant efficiency, independent of the PLR. Curve B represents equipment that is most efficient in the middle of its operating range. Curve C represents equipment that is most efficient at full load. In all cases, at very low loads (typically below 20 %), the COP experiences an intense degradation because the regulation must rely on energy-inefficient methods such as compressor cycling or hot gas by-pass.

Figure 2. (a) COP as a function of outdoor temperature (t_O) and water production temperature (t_P) (Daikin Altherma heat pump ERLQ-011-CV3 [13]) (b) Part load operation (Edwards and Finn [15]).

2.2 Terminal units' model.

The radiant floor was modelled using the component Type 705 available in TRNSYS. This component uses the finite volume method to model a slab with tubes embedded on it.

A new TRNSYS component was developed to model the fan-coil. The model is based on the effectiveness-NTU method, and it requires a value of effectiveness (ϵ) for each possible fan speed (v). This information can be easily derived from the data given in the fan-coil catalogue, applying the following equation:

$$\epsilon(v) = \frac{\dot{Q}}{\dot{Q}_{max}} = \frac{\dot{m}_{w,ct}(v) \cdot Cp_w \cdot \Delta t_{w,ct}}{C_{min} \cdot \Delta t_{max}}$$

$$= \frac{\dot{m}_{w,ct}(v) \cdot Cp_w \cdot \Delta t_{w,ct}}{min(\dot{m}_{a,ct}(v) \cdot Cp_a \,, \dot{m}_{w,c}(v) \cdot Cp_w) \cdot \left(t_{w1,ct} - t_{a1,ct}\right)}$$

Once the effectiveness is calculated, the supply air temperature t_s is given by

$$t_s = t_R + \epsilon(v) \cdot \frac{\dot{Q}_{max}}{\dot{m}_a(v) \cdot Cp_a}$$

The temperature of the water at the exit of the heating coil t_{w2} is obtained as follows

$$t_{w2} = t_P - \epsilon(v) \cdot \frac{\dot{Q}_{max}}{\dot{m}_w \cdot Cp_w}$$

Finally, the fan electricity consumption is a function of the speed and head loss in the ducts.

3. Definition of the operation modes and control

The terminal units (floor and fan-coil) work alone or simultaneously. When the fan-coil works, the fan speed can be selected among three possible levels: low, medium or high. The set-point water temperatures are 39 ^oC for the low velocity of the fan, 42 ^oC or 45 ^oC for the medium velocity and 45 ^oC for the high velocity. The set-point temperature of the production unit is 35 ^oC when the floor heating works alone. Table 1 summarizes all the feasible operating modes.

We have defined four control strategies in TRNSYS that manage the operating modes of Table 1 and the transitions between them. Table 2 shows the relationship between the control strategies that are defined in the following sections and the operating modes defined in Table 1.

3.1 RF strategy.

The RF strategy is applied when only the radiant floor operates. Figure 3 shows the scheme of this control algorithm. The control strategy is based on the change of the room dry-bulb temperature during six minutes (δ). The strategy tries to avoid overheating in both the zone and the surface of the floor. The latter is always kept below 29 ^{o}C (ISO 7730 [17] or ASHRAE Standard 55 [18]). The water temperature entering the radiant floor is 35 ^{o}C.

Figure 3. RF Control scheme.

3.2 FC1 strategy.

This strategy implements the traditional on/off control of a fan-coil. It uses only one fan velocity, usually the medium one (see Fig. 4 (a)). The hot water set-point temperature is 45 ^{o}C.

Figure 4. Control schemes for fan-coils: (a) FC1 and (b) FC2.

3.3 FC2 strategy.

This strategy is an improved version of the FC1 strategy. It modifies both the fan speed and the water set-point temperature. The control logic is illustrated in Fig. 4 (b). When the temperature of the zone is near the set-point, the control reduces the air supply in order to reduce the fan energy consumption. At the same time, the water temperature is also reduced. The opposite occurs when the thermal demand on the fan-coil increases.

3.4 CB strategy.

Figure 5 describes the CB strategy for the combined system of radiant floor and fan-coil. Some temperature ranges are defined. All fan speeds can be used and a different hot water set-point temperature is defined for each of them. In addition, the change in the zone air temperature during six minutes (δ) is monitored. Table 3 shows how the CB strategy manages the operation of the radiant floor, the fan-coil and the heat pump.

Figure 5. Scheme of the CB strategy for the combined system operation.

This control strategy aims to increase the floor surface temperature as fast as possible. During the first minutes of the system operation, the fan-coil increases the air zone temperature while the radiant floor has not the appropriate surface temperature to deal with the thermal load of the zone. Due to this, the analysis of the evolution of the zone air temperature (δ) is ignored when the set-point temperature has not been reached by the first time coming from a general shutdown. Thereby, the radiant floor remains active more time without interruption and its surface temperature increases faster.

When Δt is between -0.2 ^oC and 0.2 ^oC, the strategy has a double behaviour denoted by the temperature ranges E1 and E2. The control outputs depend on what has occurred in the previous time step. When the system comes from any temperature range in which it was able to work (either the radiant floor or the fan-coil), the control selects the state E1. Then the fan-coil is turned off and the radiant floor is activated (δ must be lower than 0.2 ^oC). On the other hand, when the system comes from the zone F (Δt < -0.2 ^oC), the system is off (E2). By doing this, we reduce the number of on-off cycles.

4. Description of the building and the systems

4.1 The building and the system.

The performance of the different control options was studied using TRNSYS 17 [12]. A living room in an intermediate plant of a residential building (see Fig. 6) was modelled using the TRNSYS Type 56 building model. The area of the plant is 44 m^2. The glazing surface is the 70 % of the window aperture.

Figure 6. Thermal zone for the case study.

Table 4 summarizes the layers of the building envelope and other data required in the simulation. Table 5 shows the thermophysical properties of each layer and Table 6 describes the parameters of the radiant floor.

We simulated the system in three locations with different heating demands and external conditions that modify the performance of the production system. The cities were: Madrid (40.45° N, 3.55° W), New York (40.78° N, 73.97° W) and London (51.15° N, 0.18° W). The weather meteorological files of EnergyPlus [19] were used. The simulation time step is two minutes.

To size the systems in each city, we calculated the peak load. The selected heat pump and fan-coils are specified in Table 7.

4.2. Performance indicators.

This work has two objectives. First, we want to evaluate the ability of the controls previously described to achieve comfort conditions in the space. As comfort indicator, we use the Predicted Percentage of Dissatisfied (PPD) which is calculated according to the ISO 7730 [17] and following the design criteria for standing or relaxed person wearing typical winter indoor clothing. Second, we want to compare the systems and control strategies during the heating season by analysing the energy consumption and the response time. The energy consumption includes the electrical consumption of the heat pump and the motor of the fans.

To these aims, we will analyse the operation and performance of the different control options on two time-scales: simulation time step (Section 5.1) and seasonal (Section 5.2).

5. Results and discussion

5.1 Hourly values.

Figure 7 shows the typical behaviour of the system when only the radiant floor is used (RF strategy). During a day of December in London, we observe the following facts:

a) Supposing that the system starts operating at 8:00, the set-point is not reached until 12:00. After 12:00, the zone air temperature is very stable, oscillating in a narrow band between 20.5 ^{o}C and 21.5 ^{o}C due to the high thermal inertia of the terminal unit.

b) The PPD is very high during the first hours of operation. From 11:00 to the end of the occupation period, the PPD is about 5 %, which is an excellent score for the radiant system.

c) The control strategy maintains the floor surface temperature below 29 ^{o}C, preventing overheating of the zone and discomfort due to high surface temperature. From 8:00 to 12:00, the heating floor is switched off two times in order to limit surface temperatures under 29 ^{o}C.

It is clear that the system has to start operating four hours in advance if the set-point conditions have to be meet when occupation begins.

Figure 7. Control strategy RF during a typical winter day in London (4th December).

Next, we will discuss the operation of the FC1 and FC2 strategies. Figure 8 shows a day of December in Madrid. Figure 8 (a) corresponds to FC1 and Fig. 8 (b) to FC2. We observe that:

a) With the FC1 strategy, which uses the medium fan velocity and a temperature of 45 ^{o}C, the system reaches the set-point temperature (21 ^{o}C) quickly. The problem with this control is that the zone temperature oscillates in a broad band between 19 ^{o}C and 22 ^{o}C due to the high level of air changes per hour caused by the fan-coil and the succession of on-off periods.

b) Using the FC2 strategy, which modifies the fan speed and the water production temperature, the results improve significantly. The band for the zone air temperature is much narrower, the time to reach comfort conditions is shorter, and the PPD is lower.

c) The PPD is frequently higher than 15 % regardless the control. Although the zone air temperature is maintained at about 21 ^{o}C, the mean radiant temperature is lower than in the case of the heating floor and the PPD is clearly higher for the fan-coil systems.

Figure 8. Control strategies FC1 and FC2 during a typical winter day in Madrid (17th December).

Finally, Fig. 9 shows the behaviour of the combined system during a day of January in New York. Compared with the previous systems and controls, the following observations can be made:

a) The set-point temperature is quickly reached thanks to the operation of the fan-coil at high speed and high temperature water (mode 5: FC-H/45).
b) The oscillation of the zone air temperature is limited within a band of ± 2.5 ^{o}C. When the floor works alone, the temperature remains almost unchanged.
c) After an initial period in which the fan-coil and the floor work simultaneously, the fan-coil is switched off and only the floor operates. The water temperature entering the floor is then reduced to 35 ^{o}C. The radiant floor works alone (mode 1: R) during 72 %, 68 % and 67 % of the time that the system is working during the heating season in London, Madrid and New York respectively.

Figure 9. Control strategy CB during a typical winter day in New York (1st January).

5.2 Seasonal results.

The controlled variable is the space dry bulb temperature, whose set-point was fixed at 21 ^{o}C. However, thermal comfort not only depends on the dry bulb temperature, but also on the mean radiant temperature. This causes differences in the comfort levels achieved by each system. Considering that the PPD has to be lower than 15 % to reach comfort [17] [18], Table 8 shows the number of hours in discomfort for each control option and city. We recall that the floor heating operates just when occupation begins.

The systems with floor heating (RF and CB) achieve better results because of the coincidence between the mean radiant temperature and the dry bulb temperature of the zone. When the radiant system works, the difference is negligible. On the contrary, the use of fan-coils exclusively (FC1 o FC2) gives mean radiant temperatures lower than dry bulb temperatures and, consequently, lower comfort levels as shown in Fig. 10.

The comfort levels can be improved for the fan-coil systems by increasing the set-point for the dry bulb temperature. We have calculated the required set-point and the increase in energy consumption required to reach the same comfort level in the simpler systems (RF and FC1). For the fan-coil system with FC1 control, the set-point temperature has to be 23.5 ^{o}C, 23 ^{o}C and 24 ^{o}C for London, Madrid and New York respectively. The increase in energy consumption compared with the original set-point was 15.9 %, 15.2 % and 17.3 % for London, Madrid and New York respectively for a type A PLR curve. These percentages do not change appreciably with curves B and C. Table 9 and Fig. 11 summarize the electric consumption of each system and control in each location. A case of heating floor with preheating was included, which avoids discomfort during the first hours of occupation.

Figure 10. Dry bulb temperature (t_R), mean radiant temperature (t_{MR}) and the Predicted Percentage of Dissatisfied (PPD) in a typical winter day in Madrid (20th January).

Figure 11. Energy consumption (kWh) for each city and control strategy.

Analysing the results of Table 9 and Fig. 11, the following conclusions can be drawn:

a) The worse system is always the fan-coil with the simplest control (FC1).
b) The best system is always the heating floor, with the exception of Madrid and New York with PLR curve type B. In these cases, the best system is the fan-coil with improved control (FC2), although the difference between both systems is small (3.7 % in Madrid and 0.2 % in New York).
c) As mentioned before, the problem with floor heating and the simplest control systems are the first hours of occupation. To avoid this discomfort period, we simulated a case in which the floor is preheated three hours before occupation. Table 9 contains a column with the electric consumption for this case. We can see that the energy consumption increases between 5.5 % and 11.6 % with respect to the best system. The combined system is the best in terms of comfort levels.
d) The PLR curve affects slightly to the energy consumption during the season. For the combined system, the differences are about 2 % depending on the PLR curve for the water heat pump. The best curve is always of type B, which presents a

maximum of COP at 50% of PLR. The mean values of PLR are shown in Table 10. The systems that use floor heating (RF and CB) achieve maximum PLR. The Table 10 also shows how the regulation of the fan velocity and the temperature of the production unit (FC2) reduce the PLR because the energy production follows better the thermal demand.

6. Conclusions

This paper analyses the operation of a heating system whose terminal units are a radiant floor and a fan-coil, and whose production unit is an air-water heat pump. The system was modelled using TRNSYS. The uncertainty in the part load efficiency of the heat pump was quantified by performing a sensitivity analysis with three different part-load performance curves. The model was used to analyse different control strategies that share the common feature of being simple to implement and having minimum hardware requirements. The RF strategy is applied when only the radiant floor operates. The FC1 and FC2 strategies are applied when only the fan-coil operates. The combined strategy CB is applied when both terminal units operate. The control decisions are only based on the zone dry-bulb temperature. The study was undertaken in three major cities with different heating requirements, in order to identify the best system and control strategy in terms of energy consumption and comfort.

The main conclusions are:

1. The radiant floor (RF) scores the lowest energy consumption except when the heat pump is most efficient in the middle of its operating range. In this case, the lowest energy consumption corresponds to the fan-coil with improved control

(FC2). The fan-coil with the simplest control (FC1) gives the highest energy consumption irrespective of the PLR curve and the weather.

2. The main drawback of the radiant floor system (RF) is the discomfort level during the first hours of occupation. This can be easily solved by activating the floor in advance. In this case, the energy consumption increases between 5.5 % and 11.6 % with respect to the best system.
3. The fan-coil systems (FC1 and FC2) report the poorest comfort level. This can be solved by increasing the temperature set-point, which will bring the comfort level near to that obtained by the systems with floor heating (RF and CB). As a result, the energy consumption of the fan-coil with the simplest control (FC1) increases between 15.2 % and 17.3 % compared to the situation with the original set-point.
4. The combined system (CB) shows the best relationship between energy consumption and comfort level. It achieves the best comfort level: the PPD is lower than 15 % during most of the time, between 94.3 % and 98.3 % of the heating season. The energy consumption is lower than in the radiant floor with preheating. It is also lower than in the fan-coil with improved control (FC2), except when the heat pump is most efficient in the middle of its operating range.
5. The most efficient system and control strategy in terms of energy consumption is independent of weather. Nevertheless, the weather has influence on the comfort: the number of discomfort hours is higher for the location with the highest heating needs.

References

[1] AHSRAE Systems and Equipment, Atlanta 2008.

[2] B. W. Olesen, Radiant floor heating in theory and practice, ASHRAE Journal 44 (2002) 19-24.

[3] B. W. Olesen, Radiant floor cooling systems, ASHRAE Journal 50 (2008) 16-20.

[4] L. Zhang, X.H. Liu and Y. Jiang, Simplified calculation for cooling/heating capacity, surface temperature distribution of radiant floor, Energy and Buildings 55 (2012) 397-404.

[5] J.M. Seo, D. Song, K.H. Lee, Possibility of coupling outdoor air cooling and radiant floor cooling under hot and humid climate conditions, Energy and Buildings 81 (2014) 219-226.

[6] A. Zarrella, M. De Carli, C. Peretti, Radiant floor cooling coupled with dehumidification systems in residential buildings: A simulation-based analysis, Energy Conversion and Management 85 (2014) 254-263.

[7] A. Afram, F. Janabi-Sharifi, Theory and applications of HVAC control systems - A review of model predictive control (MPC), Building and Environment 72 (2014) 343-355.

[8] A. Marušić, D. Lončar, Model predictive control in small family house: extravagance or future of energy consumption in households, International Federation of Automatic Control (IFAC) 48 (2015) 701–702.

[9] J. Brooks, S. Kumar, S. Goyal, R. Subramany, P. Barooah, Energy-efficient control of under-actuated HVAC zones in commercial buildings, Energy and Buildings 93 (2015) 160-168.

[10] C. Backman, A. German, B. Dakin, D. Springer, Air-to-Water Heat Pumps With Radiant Delivery in Low Load Homes, U.S. Energy Department (2013).

[11] A. Beghi, L. Cecchinato, M. Rampazzo, Thermal and Comfort Control for Radiant Heating / Cooling Systems, IEEE International Conference on Control Applications (CCA) (2011) 28-30.

[12] TRNSYS http://sel.me.wisc.edu/trnsys/. (Accessed 13.06.16).

[13] Daikin, Heating technical information Daikin Altherma ERLQ-CV3 http://extranet.daikin.es/. (Accessed 13.06.16).

[14] A.A. Safa, A.S. Fung, R. Kumar, Performance of two-stage variable capacity air source heat pump: Field performance results and TRNSYS simulation, Energy and Buildings 94 (2015) 80–90.

[15] K.C. Edwards, D.P. Finn, Generalised water flow rate control strategy for optimal part load operation of ground source heat pump systems, Applied Energy 150 (2015) 50-60.

[16] S. In, K. Cho, B. Lim, C. Lee, Partial load performance test of residential heat pump system with low-GWP refrigerants, Applied Thermal Engineering 85 (2015) 179–187.

[17] ISO 7730-2005, Ergonomics of the thermal environment. Analytical determination and interpretation of thermal comfort using calculation of the PMV and PPD indices and local thermal comfort criteria (2005).

[18] ASHRAE Standard 55, Thermal environmental conditions for human occupancy (2004).

[19] EnergyPlus, http://apps1.eere.energy.gov/buildings/energyplus/. (Accessed 13.06.16).

[20] Roca, Fan-coils RFC-RFT-RFR ftp://www.cype.net/. (Accessed 13.06.16).

Figure Captions

Figure 1. Scheme of the proposed hydronic heating system: radiant floor coupled with a fan-coil.

Figure 2. (a) COP as a function of outdoor temperature (t_O) and water production temperature (t_P) (Daikin Altherma heat pump ERLQ-011-CV3 [13]) (b) Part load operation (Edwards and Finn [15]).

Figure 3. RF Control scheme.

Figure 4. Control schemes for fan-coils: (a) FC1 and (b) FC2.

Figure 5. Scheme of the CB strategy for the combined system operation.

Figure 6. Thermal zone for the case study.

Figure 7. Control strategy RF during a typical winter day in London (4th December).

Figure 8. Control strategies FC1 and FC2 during a typical winter day in Madrid (17th December).

Figure 9. Control strategy CB during a typical winter day in New York (1st January).

Figure 10. Dry bulb temperature (t_R), mean radiant temperature (t_{MR}) and the Predicted Percentage of Dissatisfied (PPD) during a typical winter day in Madrid (20th January).

Figure 11. Energy consumption (kWh) for each city and control strategy.

Table 1. Operating modes of the system.

Mode	Radiant floor	Fan-coil	Fan speed	t_P (ºC)
0: OFF	OFF	OFF	-	-
1: R	ON	OFF	-	35
2: FC-L/39	OFF	ON	Low	39
3: FC-M/42	OFF	ON	Medium	42
4: FC-M/45	OFF	ON	Medium	45
5: FC-H/45	OFF	ON	High	45
6: R+FC-L/39	ON	ON	Low	39
7: R+FC-M/42	ON	ON	Medium	42
8: R+FC-H/45	ON	ON	High	45

Table 2. Control strategies and operating modes.

Control strategy	Terminal units		Operating modes (see table 1)
	Radiant floor	Fan-coil	
RF (section 3.1)	✓		0, 1
FC1 (section 3.2)		✓	0, 4
FC2 (section 3.3)		✓	0, 2, 3, 5
CB (section 3.4)	✓	✓	0, 1, 2, 3, 5, 6, 7, 8

Table 3. Management of the radiant floor operation, the fan-coil and the heat pump by control CB.

Temperature range (see Fig. 5)	Radiant floor	Fan-coil	Fan speed	t_P (ºC)
A	OFF	ON	High	45
B11	ON	ON	High	45
B12	If δ < 0.5 °C then ON, OFF other case	ON	High	45
B2, C1	If δ < 0.5 °C then ON, OFF other case	ON	Medium	42
C2, D1	If δ < 0.5 °C then ON, OFF other case	ON	Low	39
D2	If δ < 0.5 °C then ON, OFF other case	OFF	-	35
E1	If δ < 0.2 °C then ON, OFF other case	OFF	-	35
E2, F	OFF	OFF	-	-

Table 4. Simulation settings.

Set-point air temperature	21 °C during the occupancy period (8:00 to 23:00). Free floating temperature otherwise.			
Building envelope (starting from internal side)	External wall	Gypsum 1.5 cm / brick 9 cm / air gap 4 cm / mineral fiber rock 4 cm / brick 12 cm / mortar cement 1.5 cm		
	Interior wall	Gypsum 1.5 cm / brick 7 cm / gypsum 1.5 cm		
	Ceiling, floor	Pavement 5 cm / concrete 31 cm / pavement 5 cm		
Internal gains		Occupants [a] (people)	Lighting (W m^{-2})	Equipment (W)
	8:00 – 10:00	1	5	100
	10:00 – 16:00	1	0	100
	16:00 – 17:00	2	0	100
	17:00 – 20:00	1	5	100
	20:00 – 20:30	3	5	100
	20:30 – 23:00	4	5	100
Infiltration	Air change rate = 0.4/h			
Simulated winter period	December, January and February			

[a] *Activity level: Seated, very light writing 120 W/person (65 W sensible + 55 W latent)*

Table 5. Thermophysical properties of the massive material layers.

Layer	Thermal conductivity ($W\ m^{-1}\ K^{-1}$)	Density ($kg\ m^{-3}$)	Specific heat ($J\ kg^{-1}\ K^{-1}$)
Brick 12 cm	0.76	1600	1135
Brick 9 cm	0.49	1200	800
Brick 7 cm	0.49	1200	800
Concrete 31 cm	1.54	1168	1050
Gypsum	0.30	800	920
Mineral fiber rock	0.042	30	840
Pavement 5 cm	1.1	2000	1380
Mortar cement 1.5 cm	1.4	2000	1050

Table 6. Characteristics of the radiant floor.

Component	Parameter	Value
Floor covering (massless layer)	Thermal conductivity	2.3 W m^{-1} K^{-1}
	Thickness	8 mm
Mortar cement	Thermal conductivity	1.8 W m^{-1} K^{-1}
	Thickness	0.045 m
	Specific heat	1000 J kg^{-1} K^{-1}
	Density	2000 kg m^{-3}
Pipe	Thermal conductivity	0.35 W m^{-1} K^{-1}
	External diameter	20 mm
	Wall thickness	2 mm

Table 7. System sizing.

City	Fan-coil unit [20]						Radiant Floor	Heat pump
	Fan speed	$\dot{m}_{a,c}$ ($m^3\ h^{-1}$)	$\dot{m}_{w,c}$ ($l\ h^{-1}$)	Cap (kW)	$\dot{W}_{fan}$ (W)	$\epsilon(v)$	Pipe spacing (cm)	Model [13]
London	Maximum	1200	620	7.2	180	0.59	20	ERLQ-008-CV3
	Medium	950	520	6.0	145	0.62		
	Low	750	430	5.0	120	0.65		
Madrid	Maximum	1000	520	6.0	130	0.59	25	ERLQ-006-CV3
	Medium	800	430	5.0	85	0.61		
	Low	650	365	4.2	65	0.64		
New York	Maximum	1400	710	8.2	210	0.58	15	ERLQ-011-CV3
	Medium	1100	590	6.8	170	0.61		
	Low	850	485	5.6	135	0.65		

Table 8. Number of discomfort hours for each control and system during the heating season and the corresponding percentage.

	London	Madrid	New York
RF	103 (7.7 %)	90 (6.7 %)	152 (11.2 %)
FC1	699 (51.8 %)	506 (37.5 %)	1015 (75.2 %)
FC2	802 (59.4 %)	536 (39.7 %)	1144 (84.7 %)
CB	30 (2.2 %)	23 (1.7 %)	77 (5.7 %)

Table 9. Electric consumption (kWh) for each city and control strategy.

	RF	FC1	FC2	CB	RF+preheating
London					
A	1094	1240	1159	1126	1157
B	1072	1147	1072	1113	1138
C	1106	1288	1241	1134	1167
Madrid					
A	818	913	835	837	877
B	803	833	774	828	864
C	826	954	904	841	884
New York					
A	1518	1746	1622	1600	1625
B	1500	1634	1497	1593	1609
C	1527	1806	1729	1604	1633

Table 10. Mean values of PLR.

	London	Madrid	New York
RF	0.84	0.86	0.90
FC1	0.57	0.53	0.60
FC2	0.39	0.36	0.41
CB	0.90	0.91	0.96

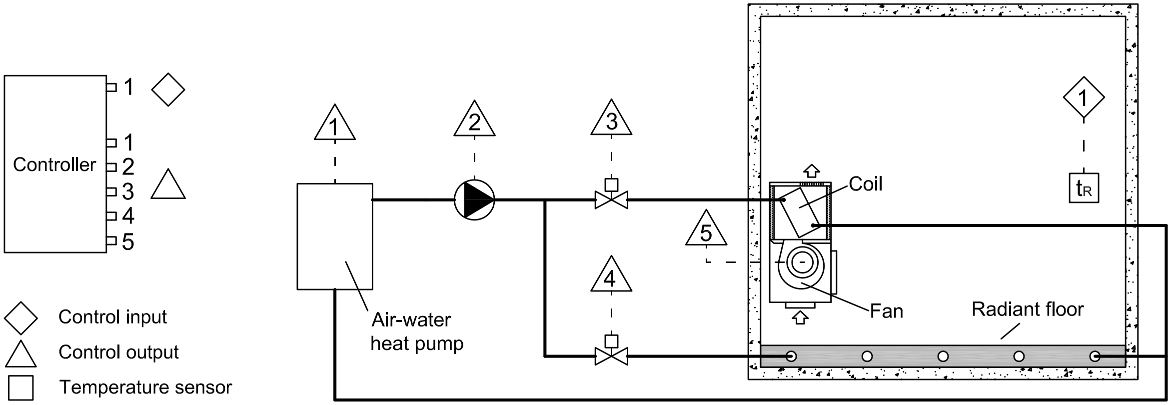

Controller
1
1
2
3
4
5
Control input
Control output
Temperature sensor
1
2
3
4
5
1
Coil
Fan
Air-water
heat pump
Radiant floor
t_R

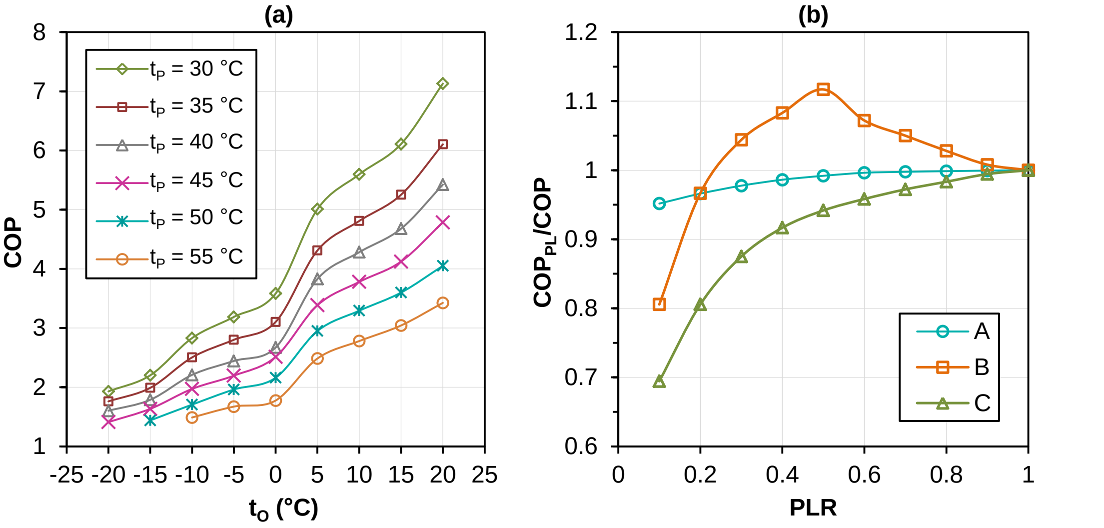

(a)
COP
8
7
6
5
4
3
2
1
-25
-20
-15
-10
-5
0
5
10
15
20
25
t_O (°C)
t_P = 30 °C
t_P = 35 °C
t_P = 40 °C
t_P = 45 °C
t_P = 50 °C
t_P = 55 °C
(b)
COP_PL/COP
1.2
1.1
1
0.9
0.8
0.7
0.6
0
0.2
0.4
0.6
0.8
1
PLR
A
B
C

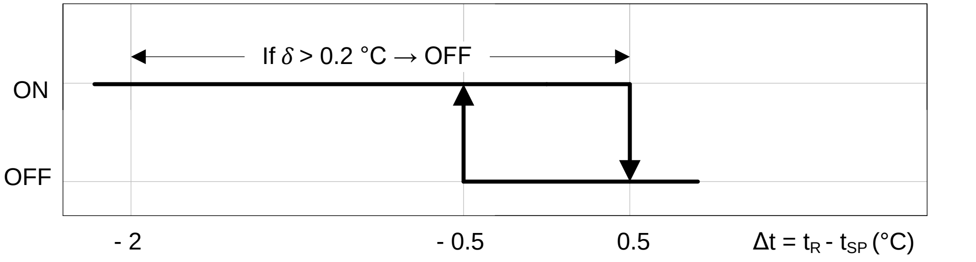
If δ > 0.2 °C → OFF
ON
OFF
- 2
- 0.5
0.5
$\Delta t = t_R - t_{SP}$ (°C)

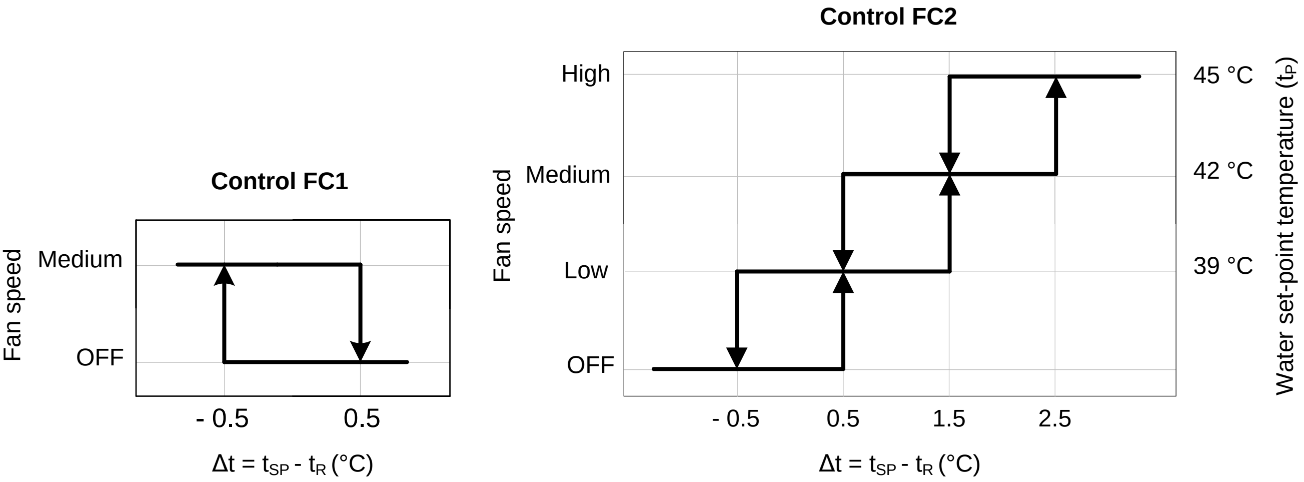

Control FC1
Fan speed
Medium
OFF
- 0.5
0.5
Δt = t_SP - t_R (°C)
Control FC2
Fan speed
High
Medium
Low
OFF
- 0.5
0.5
1.5
2.5
Δt = t_SP - t_R (°C)
45 °C
42 °C
39 °C
Water set-point temperature (t_P)

(a) (b)

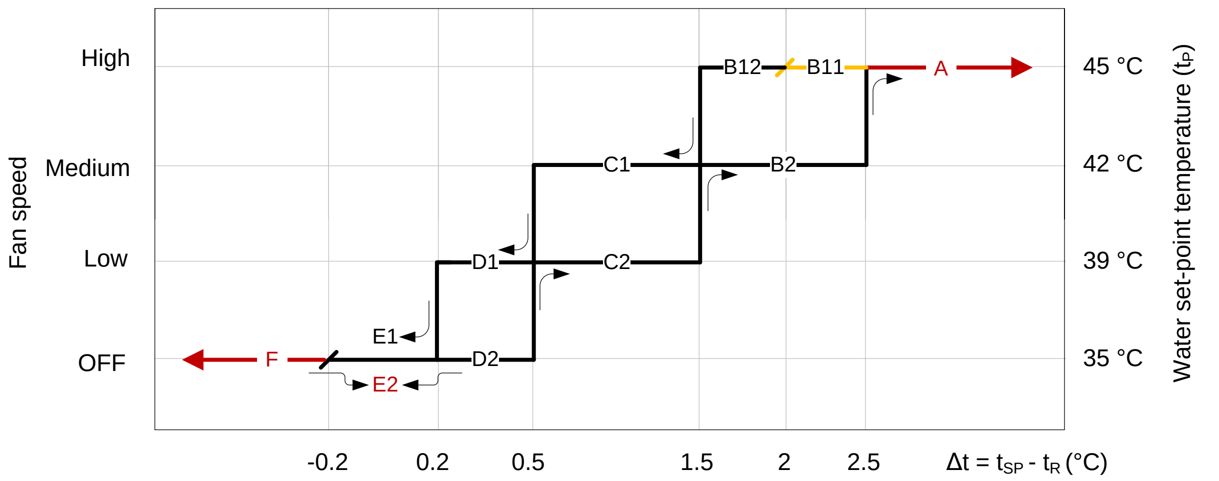

Fan speed
High
Medium
Low
OFF
B12
B11
A
C1
B2
D1
C2
E1
D2
F
E2
45 °C
42 °C
39 °C
35 °C
Water set-point temperature (t_P)
-0.2
0.2
0.5
1.5
2
2.5
$\Delta t = t_{SP} - t_R$ (°C)

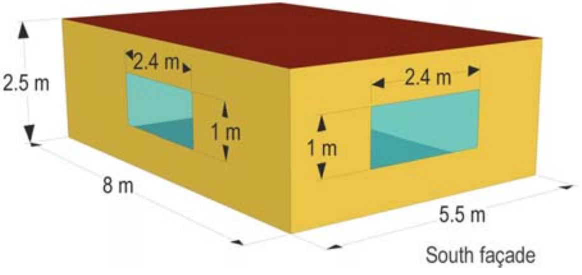
2.5 m
2.4 m
1 m
2.4 m
1 m
8 m
5.5 m
South façade

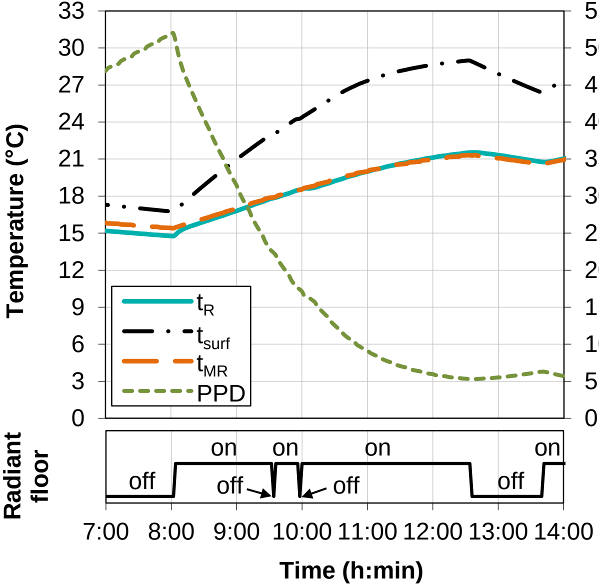
Temperature (°C)
PPD (%)
t_R
t_surf
t_MR
PPD
Radiant floor
on
off
Time (h:min)
7:00
8:00
9:00
10:00
11:00
12:00
13:00
14:00

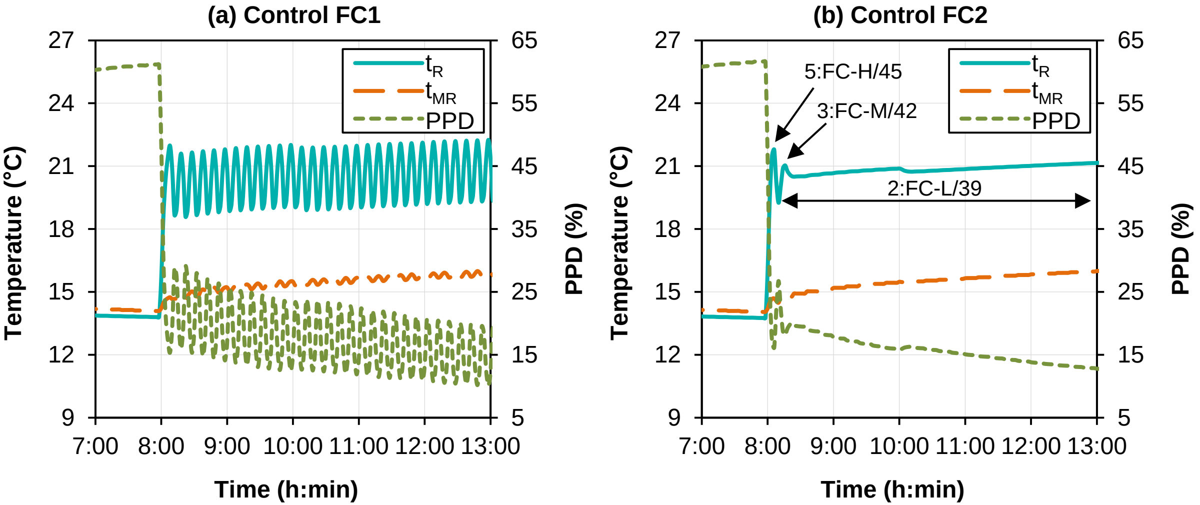

(a) Control FC1
(b) Control FC2
Temperature (°C)
PPD (%)
Time (h:min)
t_R
t_{MR}
PPD
5:FC-H/45
3:FC-M/42
2:FC-L/39
27
24
21
18
15
12
9
65
55
45
35
25
15
5
7:00
8:00
9:00
10:00
11:00
12:00
13:00

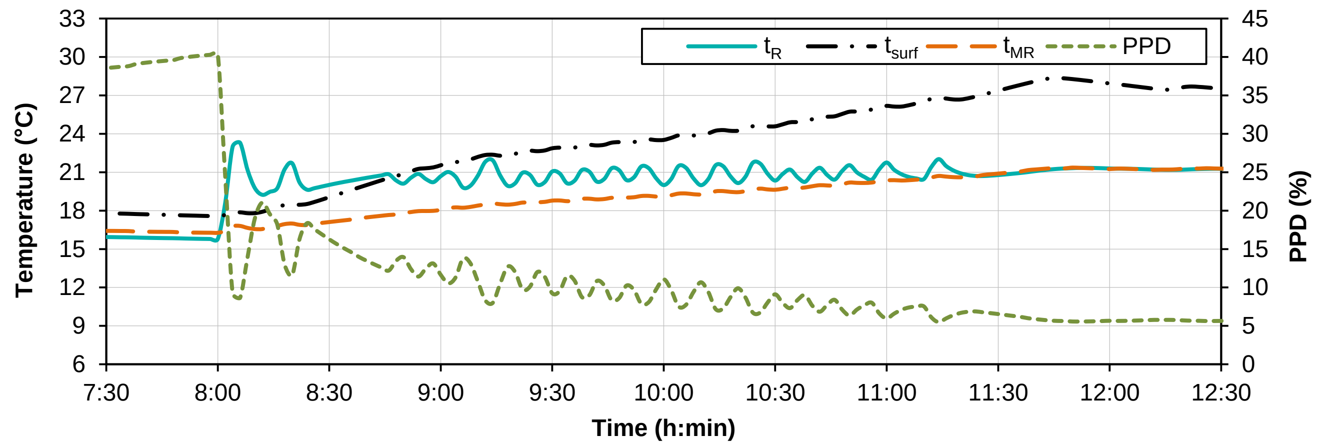

33
30
27
24
21
18
15
12
9
6
45
40
35
30
25
20
15
10
5
0
Temperature (°C)
PPD (%)
7:30
8:00
8:30
9:00
9:30
10:00
10:30
11:00
11:30
12:00
12:30
Time (h:min)
t_R
t_{surf}
t_{MR}
PPD

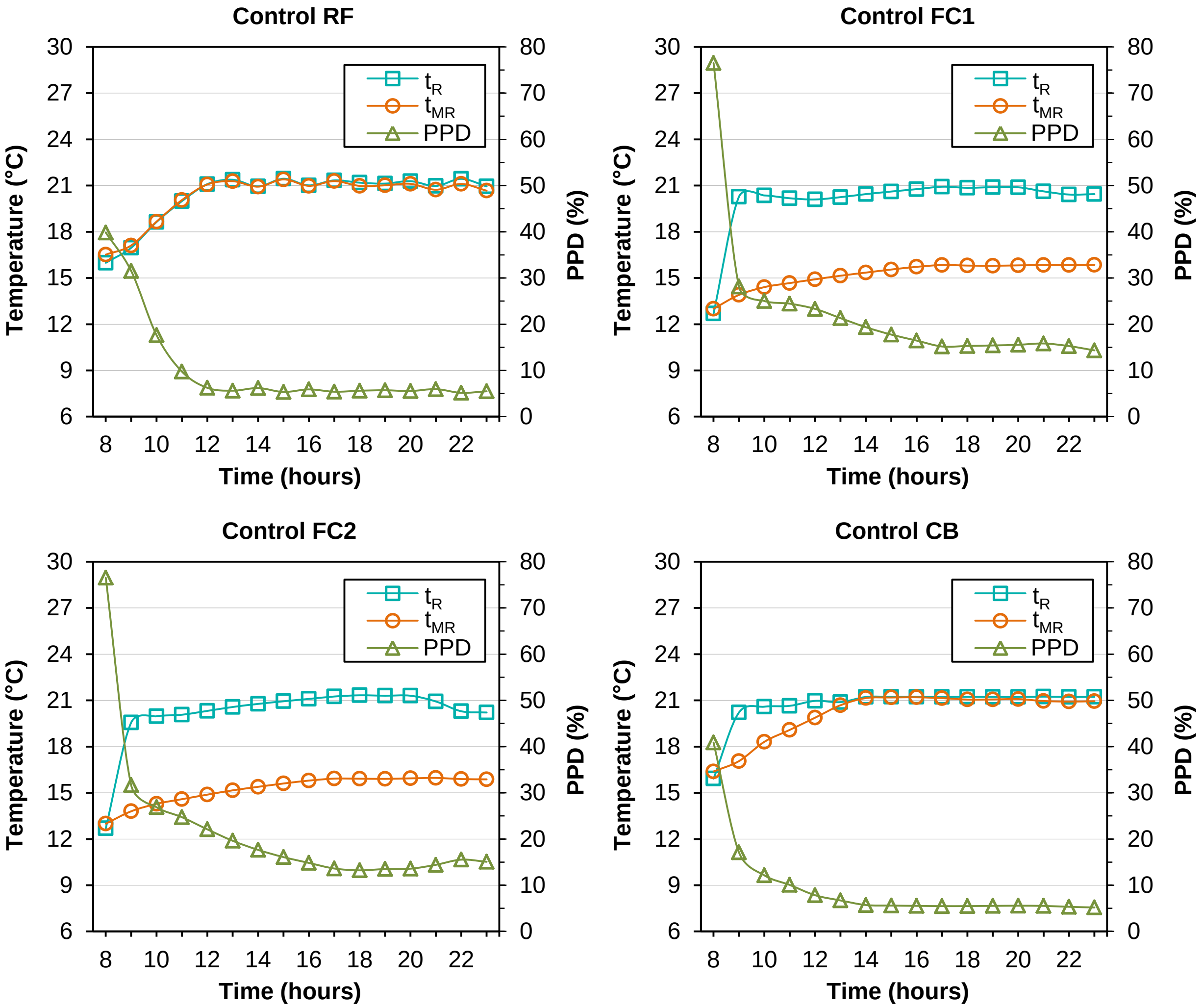
Control RF
Control FC1
Control FC2
Control CB
Temperature (°C)
PPD (%)
Time (hours)
tR
tMR
PPD
30
27
24
21
18
15
12
9
6
80
70
60
50
40
30
20
10
0
8
10
12
14
16
18
20
22

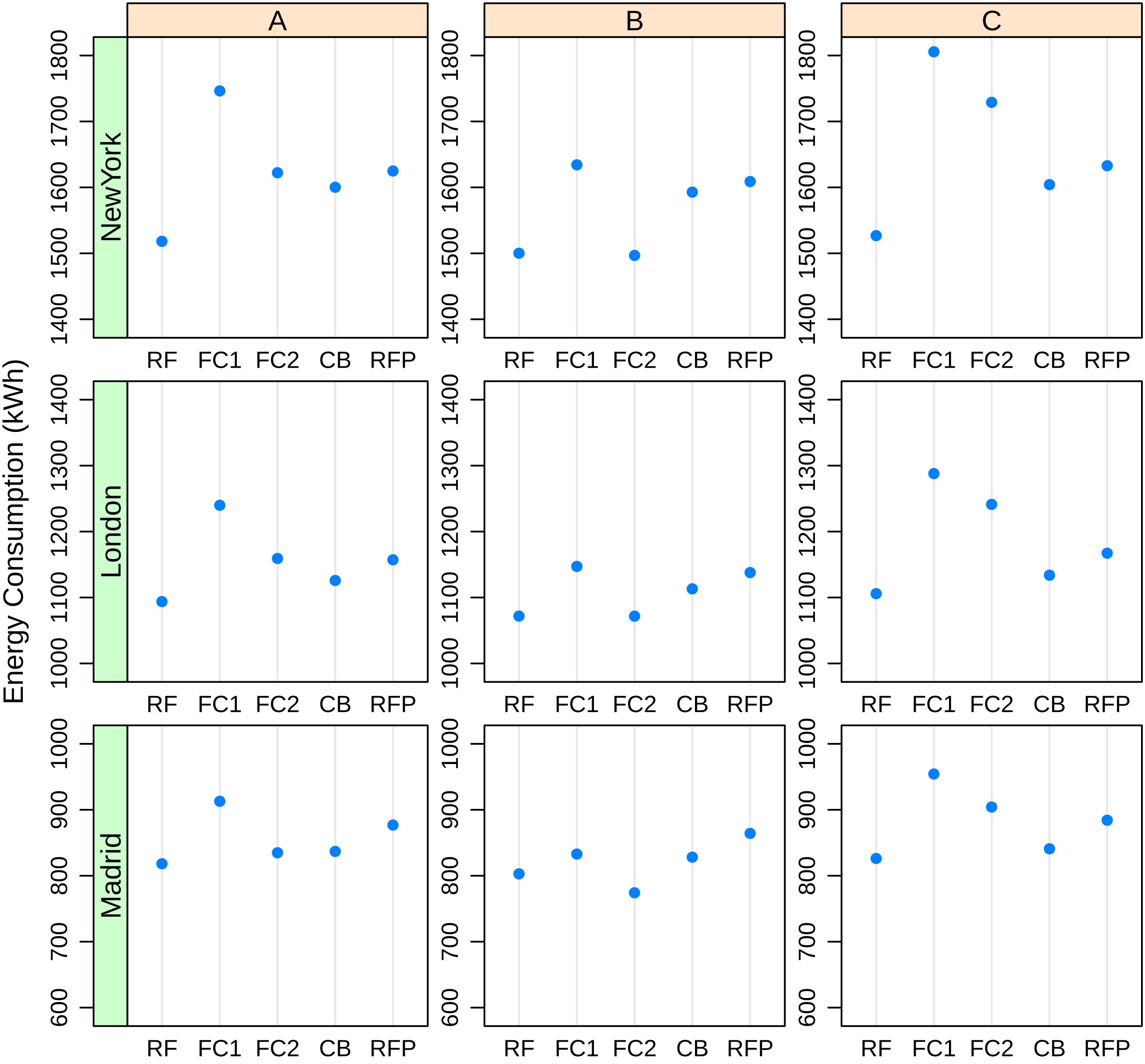
A
B
C
NewYork
London
Madrid
Energy Consumption (kWh)
RF
FC1
FC2
CB
RFP
1400
1500
1600
1700
1800
1000
1100
1200
1300
600
700
800
900